

# Machine Learning Enabled Wearable Brain Deformation Sensing System

S. Islam and A. Kim, Member, IEEE

Department of Electrical and Computer Engineering, Temple University, Philadelphia, Pennsylvania, USA  
{sayemul, albertkim}@temple.edu

**Introduction:** Brain deformation – the primary cause of traumatic brain injury (TBI) – occurs during fall, automobile accident, brain surgery, or explosion (i.e., pressurized airflow) [1]. Mechanical impact causes strain energy that leads to tissue displacement. Researchers have attempted to characterize the brain deformation for diagnosis and prevention of concussion-related TBI [2]. It is especially important to measure microscale deformation because even a few tens of micrometer brain deformation may have direct neuropsychiatric and neuro-degenerative consequences [3]–[6]. Another effort to minimize brain deformation can be found in intracranial surgeries. The deformation is inevitable but can be minimized by designing a better apparatus and using advance stereotactic techniques [7]–[9]. As such, there are a few methods to measure brain deformation today [8], [10]–[12]. Computational models and imaging technologies (e.g., FEM (finite element method) modeling, magnetic resonance imaging (MRI)) are such examples. However, because the brain is viscoelastic [13], these technologies lack 1) detailed information regarding micro-scale brain deformation and 2) real-time measurement capability.

**Method:** Our objective is to develop a novel sensing system capable of measuring microscale brain deformation in real-time. In this abstract, we report a wireless brain deformation sensing system based on the magnetic tunnel junction sensor and an implantable soft magnet combined with machine learning (ML). Figure 1(a) shows the schematic of the sensing mechanism. The magnetic tunnel junction (MTJ) sensor (Micro Magnetics, STJ-240) array can be fixed on an external fixture (e.g., helmet) and the soft magnet can be implanted under the skull. Figure 1(b-c) shows the working principle of the sensing mechanism. When the brain deforms, the soft magnet follows the brain and induces a change in the magnetic force, which can be detected by the magnetic field sensors. The brain deformation sensing system is equipped with an array of three MTJ sensors that read the change of magnetic strength due to the displacement of the implanted soft magnet [14], [15]. The soft magnets can be manufactured by mixing 40 wt% iron (III) oxide nanoparticles with silicone elastomer (Ecoflex™, 00-10) pre-gel solution and then magnetized using permanent neodymium magnets. The average magnetic field strength of the fabricated soft magnet was  $127.5\mu\text{T}$ , which was easily detectable by the MTJ sensors with pico-tesla sensitivity and well within the acceptable magnetic field strength limit for humans (400mT - 2T) [14], [16].

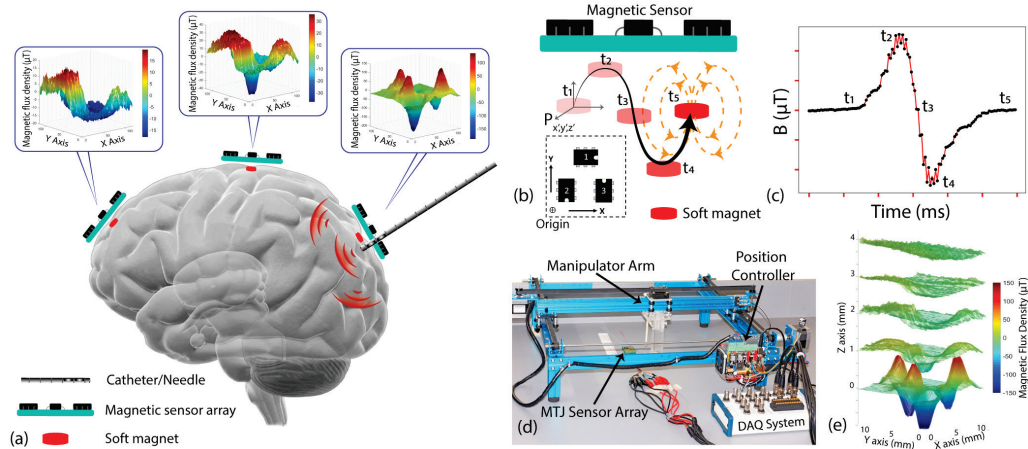


Figure 1: (a) Wireless intracranial brain deformation sensing system consists of an implantable soft magnet and an external head-mount magnetic sensor array, (b) Soft magnet displacement due to brain deformation, (c) Magnetic field strength change detected by magnetic sensors, (d) using a 2-dimensional manipulator to measure magnetic field strength along x-axis and y-axis (0 to 12 mm with 100  $\mu\text{m}$  resolution), (e) three-dimensional calibration map at  $z = 0, 1, 2, 3,$  and  $4$  mm.

We characterized the sensing behavior by creating a 3D magnetic flux density map corresponding to the position of the soft magnet. This dataset became the calibration map for training the ML system. The setup to acquire calibration data is shown in Figure 1(d). The soft magnet was mounted on a  $xy$  manipulator and the area on top of the sensor array from 0 mm to 12 mm was scanned with 100  $\mu\text{m}$  step size along  $x$  and  $y$ -axis and 0 mm to 4 mm with 1 mm step size in  $z$ -axis. The calibration data is shown in Figure 1(e). The calibration data comprised of six variables:  $x$ ,  $y$ ,  $z$  for position information and  $B_1$ ,  $B_2$ ,  $B_3$  for magnetic field strength measured by MTJ sensor array. The data set was split into two  $N \times 3$  matrices to train the ML algorithms, where  $N$  was the number of data points ( $N = 72,000$ ). The magnetic field output,  $B_1$ ,  $B_2$ ,  $B_3$  and position data of  $x$ ,  $y$ , and  $z$  were used to train the ML; and the trained ML model predicted the position data when given magnetic fields as input. Prior to the training, the sensor data were cleaned using a moving average filter. We have used three different ML algorithms: Random Forest (RF), k-Nearest Neighbor (KNN), and Multilayer Perceptron Neural Network (MLP-NN). We used RF because of its robustness and ability to work with very large dataset which can be used for both classification and regression problems [17], [18]. The KNN is one of the oldest and least complicated algorithms. It can also be used for regression problems as we have implemented. We also implemented MLP-NN to estimate the deformation. The MLP-NN mimics the simplified biological neural learning framework [19] and performs comparatively better for modeling non-linear functions and predicting from unseen data [20]. The MLP-NN network used in this study consisted of 1 input, 3 hidden and 1 output layer. The input layer has 6 nodes ( $B_1$ ,  $B_2$ ,  $B_3$ ,  $x$ ,  $y$ ,  $z$ ) and the hidden layers are a sequential cascade of 1024, 512 and 256 nodes. The output layer consists of  $x$ ,  $y$ ,  $z$  nodes as the output coordinates.

**Results and Discussion:** The ML algorithms were trained on 80% of the calibration data and the other 20% of the data were used to evaluate the performance of the ML algorithms using cross-validation. Table 1 shows the training results. Note that we calculated the normalized root mean square error (NRMSE) and R-squared ( $R^2$ ) value to compare the results. NRMSE is the normalized standard deviation of the residuals or prediction errors and  $R^2$  value is known as the coefficient of determination, often expressed in percentage value (0-100%). A significance test between the models shown that the predictions from each model were not significantly different ( $p > 0.05$ ).

Table 1. Comparison of Prediction Models and Accuracy

| ML Algorithm | Training Time (sec) | Prediction Time (sec) | NRMSE | $R^2$ (%) |
|--------------|---------------------|-----------------------|-------|-----------|
| RF           | 14.873              | 0.304                 | 0.088 | 91.3      |
| KNN          | 0.037               | 0.097                 | 0.097 | 90.4      |
| MLP-NN       | 313.69              | 0.391                 | 0.107 | 89.3      |

To further validate the brain deformation sensing technique and to demonstrate microscale deformation measurement, we used a needle insertion model using a PVC (polyvinyl chloride) gel. A soft magnet was embedded in the gel and the MTJ sensor array was placed on the surface. The experiment setup is shown in Figure 2(b). Figure 2 (a) shows time-lapse pictures during the needle insertion. We used the trained model to predict the  $z$ -axis deformation. We compared the ML results with optical measurements. Figure 2(c) compares the measured and predicted deformation. The NRMSE value between the measured deformation and predicted deformation using RF, KNN and MLP-NN were 0.069, 0.069 and 0.046 respectively and the  $R^2$  values were 96.75%, 98.16% and 98.62% respectively. The measured maximum deformation was  $2.45 \text{ mm} \pm 0.1 \text{ mm}$ , while the predicted maximum deformations were  $2.24 \text{ mm} \pm 0.168 \text{ mm}$ ,  $2.41 \text{ mm} \pm 0.168 \text{ mm}$  and  $2.23 \text{ mm} \pm 0.114 \text{ mm}$  from RF, KNN, and MLP-

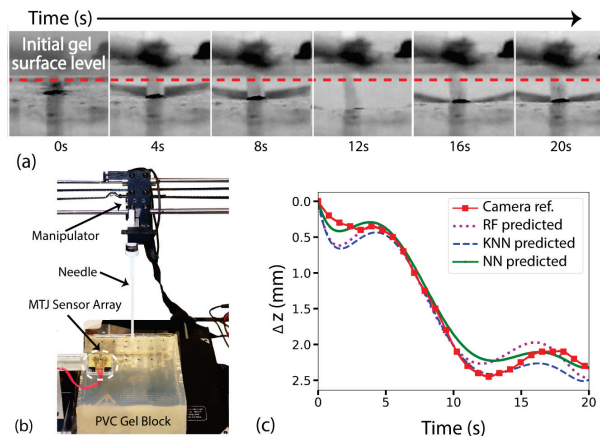


Figure 2. (a) Soft magnet displacement along  $z$ -axis in PVC gel during needle insertion test; red dashed line is drawn as reference, (b) needle insertion on PVC gel using manipulator, (c) reference position and comparison with ML predicted deformations on  $z$ -axis.

NN, respectively. The result suggests that the reported sensor system in combination with ML algorithms could measure microscale brain deformation in real-time which will bring significant impact on brain deformation and TBI research.

#### ACKNOWLEDGMENTS

This research was supported by startup funds provided by the College of Engineering at Temple University.

#### REFERENCES

- [1] "Traumatic Brain Injury (TBI)." [Online]. Available: <https://www.cdc.gov/healthcommunication/toolstemplates/entertainment/tips/BrainInjury.html>.
- [2] D. F. Meaney and Douglas H. Smith., "Biomechanics of concussion," *Clin. Sports Med.*, vol. 30, no. 1, pp. 19–31, 2011.
- [3] I. Cernak and L. J. Noble-Haesslein, "Traumatic brain injury: An overview of pathobiology with emphasis on military populations," *Journal of Cerebral Blood Flow and Metabolism*. 2010.
- [4] C. A. Taylor, J. M. Bell, M. J. Breiding, and L. Xu, "Traumatic Brain Injury–Related Emergency Department Visits, Hospitalizations, and Deaths — United States, 2007 and 2013," *MMWR. Surveill. Summ.*, vol. 66, no. 9, pp. 1–16, 2017.
- [5] J. B. Long, T. L. Bentley, K. A. Wessner, C. Cerone, S. Sweeney, and R. A. Bauman, "Blast Overpressure in Rats: Recreating a Battlefield Injury in the Laboratory," *J. Neurotrauma*, 2009.
- [6] G. A. Elder *et al.*, "Blast Exposure Induces Post-Traumatic Stress Disorder-Related Traits in a Rat Model of Mild Traumatic Brain Injury," *J. Neurotrauma*, 2012.
- [7] D. Gao, Y. Lei, and B. Yao, *Analysis of dynamic tissue deformation during needle insertion into soft tissue*, vol. 46, no. 5. IFAC, 2013.
- [8] T. Hartkens *et al.*, "Measurement and analysis of brain deformation during neurosurgery," *IEEE Trans. Med. Imaging*, vol. 22, no. 1, pp. 82–92, 2003.
- [9] A. Bzostek, R. Kumar, L. Diaz, M. Srivastava, J. H. Anderson, and R. H. Taylor, "Force vs deformation in soft tissue puncture," *Miccai*, vol. 196, 1999.
- [10] L. M. Vigneron, R. C. Boman, J. P. Ponthot, P. A. Robe, S. K. Warfield, and J. G. Verly, "Enhanced FEM-based modeling of brain shift deformation in image-guided neurosurgery," *J. Comput. Appl. Math.*, vol. 234, no. 7, pp. 2046–2053, 2010.
- [11] P. V. Bayly, T. S. Cohen, E. P. Leister, D. Ajo, E. C. Leuthardt, and G. M. Genin, "Deformation of the Human Brain Induced by Mild Acceleration," *J. Neurotrauma*, 2005.
- [12] A. K. Knutsen *et al.*, "Improved measurement of brain deformation during mild head acceleration using a novel tagged MRI sequence," *J. Biomech.*, vol. 47, no. 14, pp. 3475–3481, 2014.
- [13] K. Laksari, K. Sadeghipour, and K. Darvish, "Mechanical response of brain tissue under blast loading," *J. Mech. Behav. Biomed. Mater.*, vol. 32, pp. 132–144, 2014.
- [14] S. Cardoso *et al.*, "Magnetic tunnel junction sensors with pTesla sensitivity," in *Microsystem Technologies*, 2014, vol. 20, no. 4–5, pp. 793–802.
- [15] Micro Magnetics, "Magnetic tunnel junction sensor development for industrial applications," 2006.
- [16] G. Ziegelberger *et al.*, "Guidelines on limits of exposure to static magnetic fields," *Health Phys.*, vol. 96, no. 4, pp. 504–514, 2009.
- [17] M. H. Roy and D. Larocque, "Robustness of random forests for regression," *J. Nonparametr. Stat.*, vol. 24, no. 4, pp. 993–1006, 2012.
- [18] G. Biau, "Complete Analysis of a Random Forest Model," *J. Mach. Learn. Res.*, vol. 13, pp. 1063–1095.
- [19] S. Lek and Y. S. Park, "Artificial Neural Networks," pp. 139–194, 2013.
- [20] M. Y. Rafiq, G. Bugmann, and D. J. Easterbrook, "Neural network design for engineering applications," *Comput. Struct.*, vol. 79, pp. 1541–1552, 2001.

# MACHINE LEARNING ENABLED WEARABLE BRAIN DEFORMATION SENSING SYSTEM

Sayemul Islam and Albert Kim

{sayemul, albertkim}@temple.edu

Department of Electrical and Computer Engineering, Temple University, Philadelphia, Pennsylvania, USA

## I. Introduction

A leading cause of traumatic brain injury (TBI) is intracranial brain deformation due to mechanical impacts. This deformation is viscoelastic, differs from a traditional rigid transformation; its acceleration and direction are different from location to location. In this poster, we report a machine learning enabled wireless sensing system that allows predicting the intracranial brain deformation trajectory.

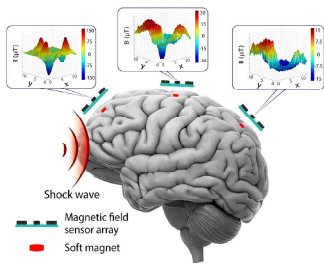


Figure 1. Schematic view of the brain deformation sensing system

## II. Methodology

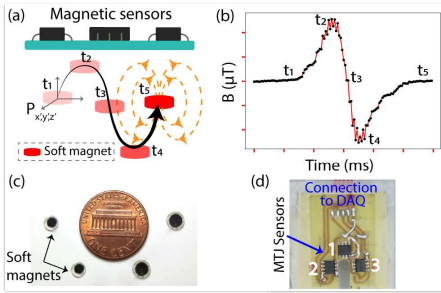


Figure 2. (a) Soft magnet displacement during brain deformation, (b) Magnetic strength change with displacement, (c) Fabricated soft magnets, and (d) The sensor array consisting three MTJ sensors

- **Sensor hardware:** Implantable soft magnet ( $\text{Fe}_2\text{O}_3$  nanoparticles in silicone elastomer (Ecoflex™) with Magnetic tunnel junction (MTJ) magnetic field sensor array.
- **Sensing mechanism:** The soft magnet implantation between the skull and the dura. The MTJ sensor array measures positions and orientations of the soft magnet during the brain deformation.

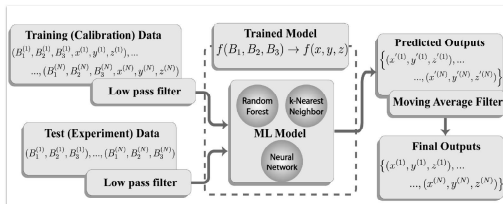


Figure 3. A process flow diagram

- **Software (Machine learning):**

**Training data:** Calibration

**Test data:** Sensor output captured during brain deformation

**Prediction:** The output of the machine learning algorithm provides the trajectory of soft magnet movement which can be translated to the brain deformation.

## III. Calibration and Training

- **Calibration:** Measured magnetic strength of five XY planes (12 mm × 12 mm) with 100 μm resolution at z = 0, 1, 2, 3, and 4 mm from the soft magnet surface.
- **ML algorithms:** RF, k-NN, and NN
- 6 variables: x, y, z, B1, B2, B3
- **Experiments:**
  - *In vitro* (needle insertion) test
  - *In vivo* (blast wave) test (dead and live rat brain)
- The results were evaluated against references (i.e., camera measurement and previously developed empirical models).
- **Validation parameters:** Absolute error, RMSE, Pearson's R, and R<sup>2</sup>

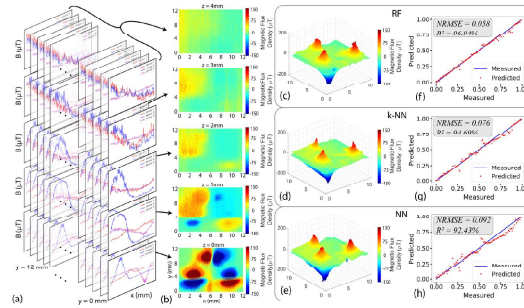


Figure 4. Data structure: (a) sensor output, (b) calibration data of measured magnetic strength in five XY plane, (c-e) reconstructed 3D calibration using RF, k-NN and NN, (f-h) correlation results

## IV. Results - In Vitro

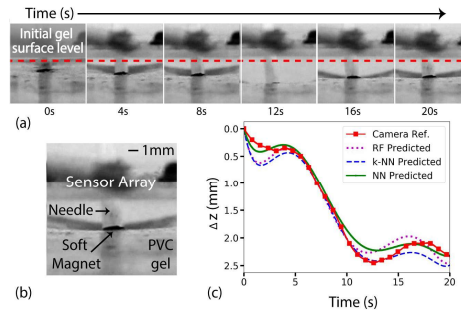


Figure 5. (a) Soft magnet displacement along z-axis in PVC gel during direct mechanical stimulation, (b) soft magnet and sensor array location, (c) relative comparison of deformation captured by camera with ML predicted results along z axis

### In Vitro Experiment using Gel phantom

- Soft magnet was implanted in PVC gel
- Sensor array was placed 2 mm above the gel surface
- Needle was inserted into next to the soft magnet
- High speed camera was used to measure the gel deformation as a reference.
- Greater than 95% R<sup>2</sup> using all ML algorithms (Table I)

| Comparison              | ML algorithm | Avg. Abs. Err (μm) | NRMSE | Pearson Corr., R | R <sup>2</sup> (%) |
|-------------------------|--------------|--------------------|-------|------------------|--------------------|
| PVC gel (Camera vs. ML) | RF           | 137.4              | 0.069 | 0.984            | 96.75              |
|                         | k-NN         | 128.9              | 0.069 | 0.991            | 98.16              |
|                         | NN           | 90.0               | 0.046 | 0.993            | 98.62              |

## V. Results - In Vivo

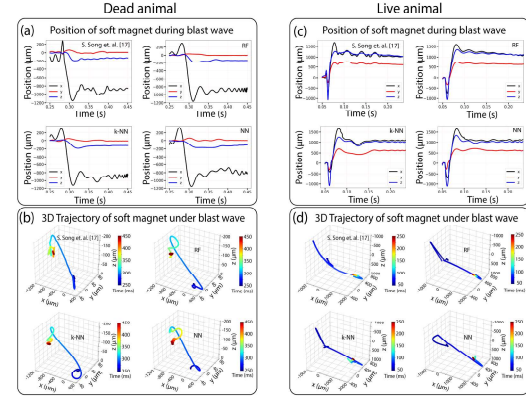


Figure 6. Deformation for (a-b) dead and (c-d) live rat brain

### In Vivo Experiment using rat brain

- Intracranial brain deformation due to blast wave
- Test specimen: Dead and live rat brain.
- Implanted soft magnet and placed a sensor in a helmet.
- The sensor data were processed using both previously developed empirical model [1] and the ML models.
- Predicted deformations have very high correlation with the calculated deformation (Table II)

| Comparison                    | ML algorithm | Avg. Abs. Err (μm) | NRMSE | Pearson Corr., R | R <sup>2</sup> (%) |
|-------------------------------|--------------|--------------------|-------|------------------|--------------------|
| Dead rat (Gaussian vs. ML)    | RF           | 41.1               | 0.126 | 0.777            | 68.20              |
|                               | k-NN         | 37.0               | 0.120 | 0.880            | 79.32              |
|                               | NN           | 50.0               | 0.117 | 0.883            | 78.75              |
| Live rat (Gaussian vs. ML)    | RF           | 82.0               | 0.078 | 0.928            | 86.22              |
|                               | NN           | 98.0               | 0.074 | 0.933            | 87.02              |
| Calibration (Gaussian vs. ML) | RF           | 576.6              | 0.085 | 0.902            | 81.42              |
|                               | k-NN         | 713.9              | 0.105 | 0.893            | 79.65              |
|                               | NN           | 752.5              | 0.114 | 0.818            | 66.94              |

## VI. Conclusion

The sensing system provides a practical solution to characterize the traumatic mechanical event by combining magnetic sensing mechanism and machine learning. It will allow for testing hypotheses regarding pathogenesis post-TBI neuropathology that have been largely speculated and it will enlighten potential methods for injury prevention, diagnosis, and treatment.

## VII. Acknowledgements

This research was supported by startup funds provided by the College of Engineering at Temple University. Authors would also like to thank S.T.R. Gidde and Moonchul Park for their time and expertise during the experiment and data collection.

## VIII. References

- [1] Song, S., N. S. Race, A. Kim, T. Zhang, R. Shi, and B. Ziaie. "A wireless intracranial brain deformation sensing system for blast-induced traumatic brain injury." Scientific reports 5 (2015): 16959.